Journal of Ovonic Research Vol. 12, No. 2, March - April 2016, p. 113 - 120

PHONONS LATTICE DYNAMICS AND TRANSPORT PROPERTIES OF MULTIFERROIC $LaFeO_3$

M. TUFIQ JAMIL[a*], J. AHMAD[a], M. SALEEM[b], S. M. RAMAY[c]
[a]*Solid State Spectroscopy Laboratory, Department of Physics, Bahauddin Zakariya University, Multan 60800, Pakistan*
[b]*Department of Physics, Syed Babar Ali School of Sciences and Engineering (SBASSE), Lahore University of Management Sciences (LUMS), Opposite Sector U, DHA, Lahore 54792, Pakistan.*
[c]*College of Science, Department of Physics and Astronomy, King Saud University, Riyadh, Saudi Arabia.*

Successful synthesis of single phase multiferroic $LaFeO_3$ and its lattice dynamic study is presented. The $LaFeO_3$ has been synthesized by sol-gel auto combustion citrate method. Powder of the sample sintered at 900 ^{0}C, resulted in well crystalline orthorhombic single phase $LaFeO_3$ as identified by X-ray diffraction (XRD) analysis. Crystallite size estimated by Debby Scherrer formula is in the range of 100 nm. Normal incident reflectivity spectra obtained at room temperature in the frequency range 30-7500 cm^{-1}possess well resolved optical phonon. Typical insulator like reflectivity spectra have been observed and discussed in terms of phonon dynamics and its possible role in multiferroic properties for $LaFeO_3$.

(Received February 17, 2016; Accepted April 13, 2016)

Keywords: Phonon dynamics; transport properties; multiferroic

1. Introduction

Rare earth orthoferrites (R_eFeO_3) with orthorhombic perovskite structure have attracted both researchers and technologists due to their unique and exciting chemical and physical properties [1, 2], and its considerable applications, such as solid oxide fuel cells [3], catalysts [4, 5], gas sensors [6] and environmental monitoring applications [7]. In $LaFeO_3$, 3d electronic configuration is responsible for magnetic ordering in material with transition metal ions, produce a lattice distortion due to which strong local electric field is created. Due to this locally induced field, ferroelectric ordering developed in this type of materials. A number of compositions with perovskite type of structure were found where long range orderings of spin configuration (ferro/ferri-magnetic and/or antiferromagnetic) and dipole moments (ferroelectric and antiferroelectric) were observed [8]. Among the rare-earth orthoferrites, lanthanum orthoferrite ($LaFeO_3$) is a very well known antiferromagnetic material with high value of Néel temperature (T_N~740 °C) [9,10]. Among this family, $LaFeO_3$ is a class of material, which has a distorted perovskite structure with a space group *pbnm* [11, 12]. It possesses magnetic as well as ferroelectric ordering and this is a so called multiferroic (MF) material [13, 14]. Recently, various investigations regarding antiferromagnetism, exchange bias-effect, electronic structure and hyperfine properties of bulk and thin film of $LaFeO_3$ have been studied [15,16]. Coupling between magnetic and ferroelectric order and its possible effects on the physics of the $LaFeO_3$ is still not fully investigated. Local vibrations of various elements involved i.e. La, Fe and O can be studied through measuring optical phonon, which can provide information regarding coupling of both orders for better understanding of the multiferrocity in the systems like $LaFeO_3$.

Here we present optical reflectivity spectra of $LaFeO_3$ in the infrared region and studied optical phonons. We will also discuss the results of structural, optical, electrical, dielectric and

*Corresponding author : tufiqjamil@yahoo.com

magnetic measurements of $LaFeO_3$ prepared by combination of sol-gel autocombustion citrate method.

2. Experimental Methods

Polycrystalline $LaFeO_3$ was synthesized by sol-gel auto combustion method. Sol-gel method is adopted for synthesizing $LaFeO_3$ in the present work take to the fact that it is a low temperature synthesis process and provides more homogeneous, less porous samples with controlled particle size. In synthesis process 50 ml of one mole lanthanum nitrate hexahydrate $La(NO_3)_3.6H_2O$ solution was added to 50 ml of one mole iron nitrate nanohydrate $Fe(NO_3)_3.9H_2O$. One mole monohydrate citric acid $C_6H_8O_7.H_2O$ in 50 ml deionized water was also mixed in above raw materials as a chelating agent. Metal nitrates to citric acid ratio were kept at 1.5:1. pH of the solution was adjusted at 7 by adding proper amount of ammonia solution(85% deionized water and 15% ammonia) during stirring process drop wise. The resulting aqueous solution was continuously stirred and heated at constant temperature of about 80^0C. Due to evaporation, solution was converted into viscous gel after 2 hours. A fine powder was obtained after an intense exothermic combustion reaction. The resulting powder was sintered at 900 ^{0}C for 3 h in a muffle furnace in an ordinary environment. The phase identification was carried out using (Bruker D8 advance) X-ray diffractometer (XRD) equipped with Cu source of X-rays of wavelength 1.54 Å. Average grain size was calculated by Scherrer's formula considering the position and broadening of the most intense diffraction peak in XRD spectra. Morphology and composition of the sample were observed using FEI NOVA 450 scanning electron microscope (SEM) equipped with Oxford energy dispersive X-rays spectroscopy (EDS) detector. The UV-Visible absorption technique was used to measure the optical band gap. Temperature dependent electrical resistivity was measured using four point probe setup. The frequency dependent dielectric properties were obtained in frequency range 100 Hz to 1 MHz, using LCR meter (model 1920 precision). Magnetic properties were measured by Physical Properties Measurement System (PPMS) magnetometer. FTIR reflectivity spectrum was taken by Fourier transform infrared spectrometer (Bruker Vertex 80v) in the frequency range 30–7500 cm^{-1} at room temperature. This frequency range has been covered using KBR-DLaTGS and Mylar 6 µm DLaTGS beam splitter-detector combination.

3. Results and discussion

Fig. 1 shows the XRD spectra of polycrystalline $LaFeO_3$. The diffraction peaks of powder sample are very narrow and sharp, which show high crystallinity. All peaks of the pattern assigned to $LaFeO_3$ according to JCPDS card No. 74-2203, suggest orthorhombic perovskite structure with space group *pbnm* (No. 62), no impurity peaks observed guarantees formation of single phase $LaFeO_3$. The lattice parameters calculated are a = 5.553Å, b = 5.563Å and c = 7.867Å. The average crystallite size of as prepared $LaFeO_3$ is 100 nm which was calculated by the Scherrer's formula [$D = 0.89\lambda/\beta\cos\theta$, where λ is the wavelength of X-ray radiation (1.54056 Å), θ is the diffraction angle and β is the full width at half maximum (FWHM) of diffracted peaks].

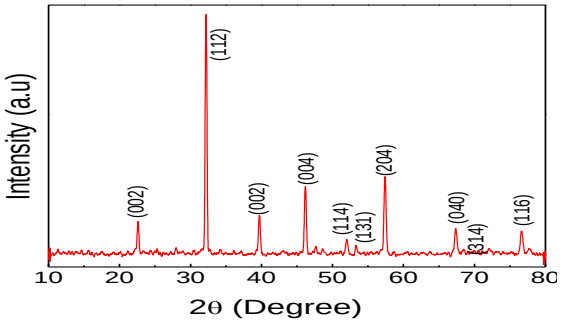

Fig.1: XRD pattern of as prepared $LaFeO_3$.

Fig. 2 shows the SEM micrograph of $LaFeO_3$ sample which was taken at 10 kv accelerating voltage and magnification of 80k. Large grains with less grain boundaries can easily be seen from micrograph. However, grains show no perfect alignment, which is a typical characteristic of polycrystalline sample. The individual particles shown in the figure are of the round shape with an average particle size 100nm, which is consistent with XRD results.

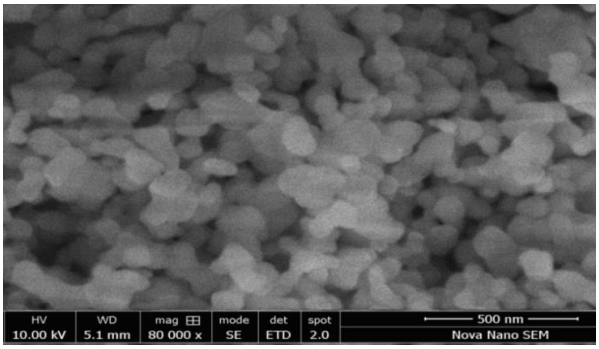

Fig 2: SEM micrograph of $LaFeO_3$.

In Fig. 3, EDX spectra show the chemical composition of the synthesized $LaFeO_3$. It can be seen that there are clear peaks of lanthanum, iron, and oxygen elements present in the synthesized sample with the molar ratio of about 1:1:3 (La:Fe:O), giving a stoichiometric formula $LaFeO_3$. There is no peak of other impurity elements which confirms the phase and composition purity of the sample. Single peak of carbon appeared is due to carbon tape on which sample was mounted with holder.

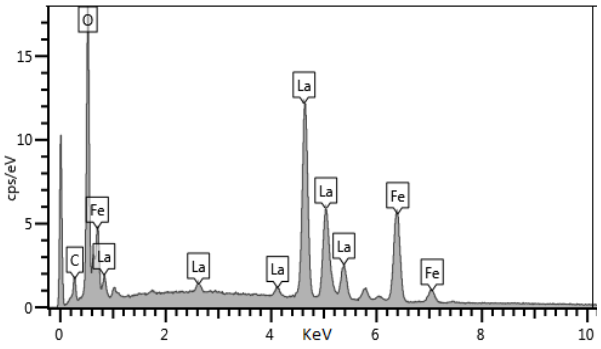

Fig.3: EDX analysis of the synthesized perovskite lanthanum orthoferrite.

UV-visible spectroscopy has been employed to analyze the optical behavior of polycrystalline $LaFeO_3$. Fig. 4 shows absorbance spectrum of $LaFeO_3$ in the wavelength range 210~700 nm at room temperature. Absorbance seems to drastically decrease in the visible wavelength range, i.e. 600 ~ 450 nm, followed by no change up to around ~380 nm. Afterward, a clear absorption peak centered at ~343 nm appears in the spectrum. This latter absorption peak may be associated to energy band gap between O-2p valance band and Fe-3d conduction band, which is estimated to be ~3.62 eV. This value of band gap suggests $LaFeO_3$ as a UV absorber and act as an insulator.

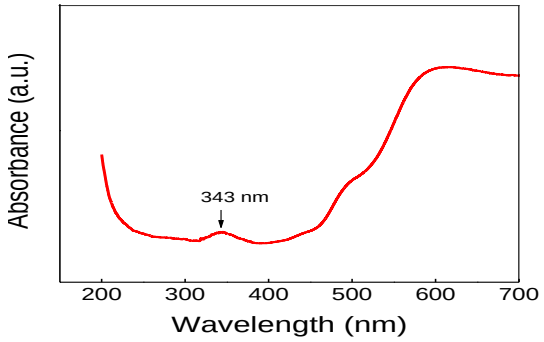

Fig.4: UV- Visible spectrum of $LaFeO_3$ nanocrystals.

Fig. 5 shows the temperature dependent resistivity of $LaFeO_3$. It is obvious from the result that the resistance of the material remains almost constant from room temperature to 120 ^{0}C, suggesting an insulating behavior of the material. But above 120 ^{0}C resistivity increases with rise in temperature showing metallic behavior. Generally, the electrical conduction in thermally activated transition metal oxides are due to electron and/or hole hoping between same transition metal cations of different oxidation states (electronic conduction) or hoping of oxygen vacancies in oxygen deficient oxides. However, the electrical conduction in $LaFeO_3$ in the measured temperature range from room temperature to 240 ^{0}C is entirely due to electronic conduction. These results show that La is only in trivalent state but Fe exist in trivalent (Fe^{3+}) and tetravalent (Fe^{4+}) oxidation state with high spin state electronic configurations [17]. In short, the electrical conduction in $LaFeO_3$ is due to holes hoping between Fe^{4+} and Fe^{3+}. This result of hole hoping between Fe^{3+} and $Fe^{4+}$is in accordance with a previous report of Iwasaki *et. al.* [18]. As it is concluded above that the mobility of hole hoping between Fe^{4+} and Fe^{3+} increases with temperature therefore, the observed shift towards metallic behavior at higher temperature is expected.

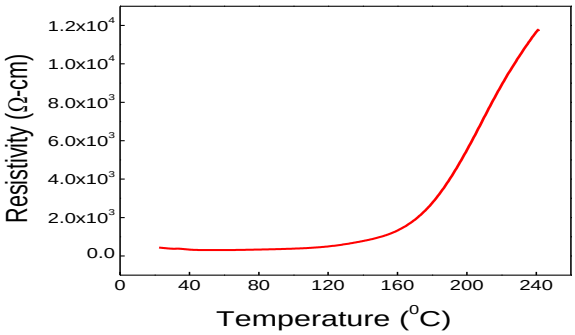

Fig. 5: Temperature dependent resistivity of the perovskite $LaFeO_3$ measured during cooling in steps of 20 ^{0}C between room temperature and 240 ^{0}C.

Frequency dependent dielectric constant $\varepsilon^* = \varepsilon^{/} - i\varepsilon^{//}$ is measured in frequency range 100 Hz to 1 MHz as shown in Fig. 6. The appreciable high value of real dielectric constant $\varepsilon^{/}$ shows large polarization of atoms and their easy charge transport phenomenon through well ordered chain of molecules in crystal structure as it was described by Joo *et. al.* [19]. The decrease in dielectric constant at higher frequency is well explained by Debye's effect. According to Debye, a material contains atoms, molecules or group of atoms which turn into dipoles on the application of electric field. When the frequency of the electric field increases, the polarization of the material decreases due to deformation and change in orientation of the dipoles and vanish when frequency becomes sufficient high [20]. When the electric field is removed the polarization decay with time due to reorientation of the dipoles according to equation

$$p(t) = p_o \exp(-t/\tau) \quad (1)$$

Where p_o is a constant and τ is the relaxation time for the polarization to be reduced to *1/e* of its original value. Since, relaxation involves rotational rearrangements there are energy barriers associated with the process related to the energy (H) by the equation

$$\tau = \tau_o \exp\left(\frac{-H}{KT}\right) \quad (2)$$

where τ_0 is a constant and k is a Boltzmann's constant, τ is further related to the frequency at which maximum loss occurs (f_m), for a given relaxation can be described by the equation

$$\tau = \frac{1}{2\Pi f_m} \quad (3)$$

The frequency dependence of the complex dielectric constant can be expressed by the Debye equation. Polarization generally exists due to reversal of the electric dipoles with the applied frequency. In $LaFeO_3$ hole hoping between Fe^{4+} and Fe^{3+} can be responsible for the dipolar polarization. The dielectric constant at low frequencies, ($f < f_r = 1/2\pi\eta r$), where the electric dipoles follow the variation in the applied ac electric field, is called the corresponding static dielectric constant. As frequency increases, the motion or reversal of the dipoles is limited by the mobility of the electric dipoles and they lag behind the applied field. Consequently, **ε** decreases, when the variation in the applied ac electric field reaches those of the relaxation frequency ($f_r = 1/2\pi\eta r$) and above this frequency, electric dipoles are not mobile enough to follow the applied ac electric field. As the frequency is increased the interfacial dipoles and orientation polarization of dipoles cannot follow the external electric field and therefore leads to the decrease of dielectric constant so the value of $\acute{\varepsilon}$ and ε'' decreases with the increase of frequency. As a consequence, the dielectric constant decreases sharply and remains almost constant at higher frequencies as depicted in Fig. 6.

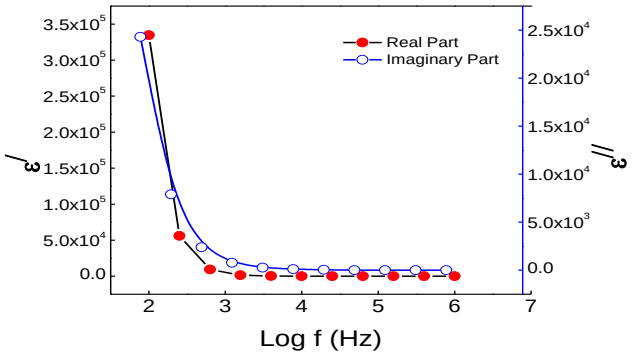

Fig.6:Frequency dependent real and imaginary parts of dielectric constant of $LaFeO_3$.

We have analyzed the magnetic behavior of as prepared $LaFeO_3$in the magnetic field range of ±10kOe. As shown in Fig. 7, the M(H) hysteresis loop of $LaFeO_3$ at room temperature corroborated the presence of clear magnetization. The system $LaFeO_3$ is found to be an antiferromagnetic material and all antiferromagnets are either semi-conductors or mostly insulators [16,18]. This also implies absence of any free charge carriers in $LaFeO_3$ and the electrons responsible for their magnetic properties are localized. It seems to be the combined behavior of dual contributions of paramagnetic and antiferromagnetic interactions. However, coercivity is somewhat high from the expected values, which is associated with the different structural aspect produced due to different type of preparation techniques. This high coercivity can be useful in some applications required for the combination of insulating materials with high coercive field.

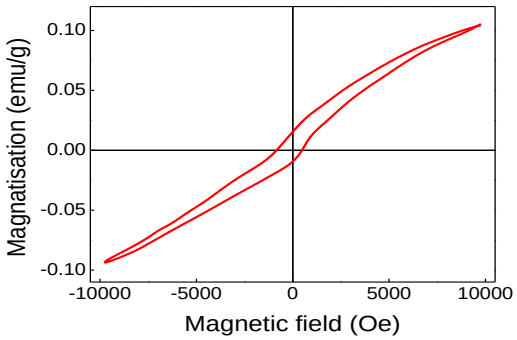

Fig.7:Room temperature magnetic behavior of $LaFeO_3$.

The reflectivity spectrum of $LaFeO_3$in the frequency range of 30-800 cm^{-1} at room temperature is shown in Fig. 8. The spectrum above frequency range 800 cm^{-1} was structure less, so not included here. The five phonon peaks can be clearly seen in the reflectivity spectra.

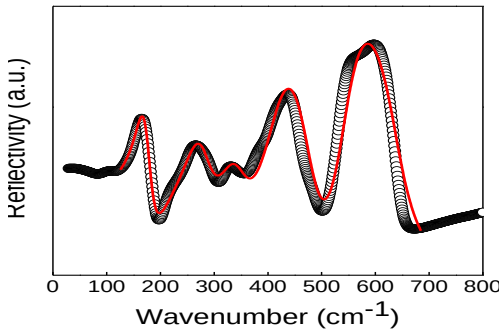

Fig.8:Reflectivity spectrum of $LaFeO_3$ at room temperature. Open circle and solid lines show the experimental and fitted spectra respectively.

We fit the Lorentz oscillator model to reflectivity spectrum for quantitative analysis. According to this model, the dielectric function *ε (ω)* is defined as

$$\varepsilon(\omega) = \varepsilon_\infty + \frac{\omega_{TO(j)} S_j}{\omega_{TO(j)} - \omega^2 - i\omega\gamma_j} \quad (4)$$

and related to reflectivity *R(ω)* as

$$R(\omega) = \left| \frac{1-\sqrt{\varepsilon(\omega)}}{1+\sqrt{\varepsilon(\omega)}} \right|^2 \quad (5)$$

where, ε_∞ is the high frequency dielectric constant, $\omega_{TO(j)}$, S_j and γ_j are the phonon frequency, oscillator strength and the damping factor of j^{th} transverse optical (TO) phonon, respectively. The parameters extracted from best fit are tabulated in Table 1.

Table 1: Different parameters of FTIR reflectivity for $LaFeO_3$.

ε_∞	Phonon modes	$\omega_{TO,j}$	$\omega_{LO,j}$	γ_j	S_j
1.35	1	168	184	30	0.81
	2	271	295	59	0.68
	3	335	356	68	0.38
	4	415	482	78	0.65
	5	539	640	65	0.22

The first phonon mode at 168 cm^{-1} involves the motion of La atoms relative to FeO_6 octahedra, because La atom heavier in $LaFeO_3$ system vibrates at low frequency. Moreover, the phonon modes at 271, 335, and 415 cm^{-1} correspond to the complex motion of Fe atoms, relative to the displacement of oxygen atoms. High frequency mode at 539 $cm^{-1}$is assigned to motion of oxygen atoms relative to Fe. The phonon frequencies at intermediate range are expected to give rise splitting of the bending and stretching modes of ideal perovskite structure. In the reflectivity spectrum of $LaFeO_3$, several kinks observed above 270 cm^{-1}, reflect strong orthorhombic distortion in the ideal perovskite structure but we cannot classify any mode as purely bending or stretching. However these modes greatly affect the changes of both Fe-O bond lengths and Fe-O-Fe bond angle. In Fig. 9 (a), the peak positions in the imaginary part of dielectric function (Im(ε)) and the loss function (Im(-1/ε)) correspond to transverse optical (TO) and longitudinal optical (LO) modes, respectively. For quantitative analysis of phonon contribution to the infrared spectrum of $LaFeO_3$, we have calculated the optical conductivity $\sigma(\omega) = \omega\varepsilon_2/4\pi$, and plotted in Fig. 9 (b). The optical conductivity $\sigma(0)$ is zero suggesting no contribution of free charge carriers at low frequency, thus demonstrating insulating behavior of $LaFeO_3$.

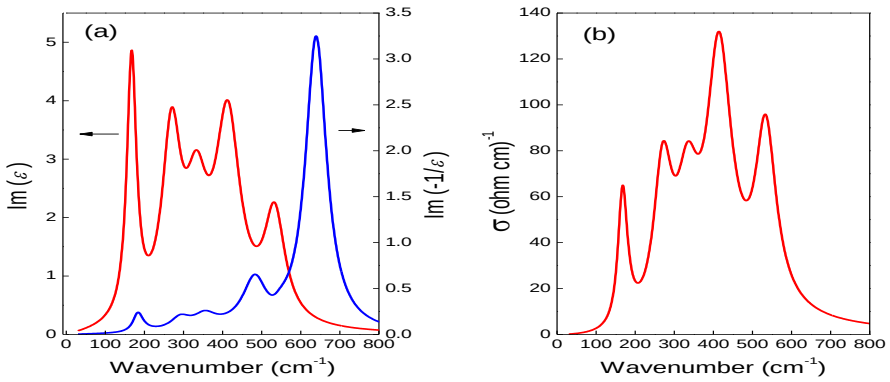

Fig.9: (a) Imaginary part Im(ε) of dielectric function and loss function Im(-1/ε) of prepared $LaFeO_3$. (b) Optical conductivity of $LaFeO_3$.

4. Conclusions

Single phase orthorhombic $LaFeO_3$ was synthesized by using sol-gel method. The crystallite size estimated as 100 nm is consistent with the SEM analysis and chemical composition in the ratio (1:1:3) was confirmed through EDX. Insulating behavior has been observed by high resistivity and band gap of about 3.62 eV was also estimated by UV-visible absorption spectra. It also exhibits strong dielectric mechanism and antiferromagnetic ordering has been assumed through their magnetic behavior. Infrared reflectivity spectra of $LaFeO_3$ have been obtained in the frequency range 30 - 800 cm^{-1} by using FTIR reflectivity spectroscopy. One of the interesting consequences is the detection of five active phonon modes at 168, 271, 335, 415 and 539 cm^{-1}. These observed results show that $LaFeO_3$ is a strong candidate for photo catalyst and can also be used for dielectric purpose.

Acknowledgement

One of the authors (Shahid M. Ramay) would like to extend his sincere appreciation to the deanship of scientific research at King Saud University for funding No. RG 1435-004.

References

[1] J. Li, X. Kou, Y. Qin,H. He, Journal of Applied Physics **92**, 7504 (2002).
[2] M. B Bellakki, V Manivannan, Bull. Mater. Sci. **33**, 611 (2010).
[3] D. Kuscer, M. Hrovat, J. Holc, S. Bernik, D. Kolar, Journal of Power Sources **61**, 161 (1996).
[4] D. Fino, N. Russo, G. Saracco,V. Specchia, Journal of Catalysis **217**, 367 (2003).
[5] T. Selyama, N. Yamazoe, K. Eguchl, Ind. Eng. Chem. Prod. Res. Dev. **24**, 21 (1985).
[6] D. Wang, X. Chu, M. Gong, Nanotechnology **17**, 5501 (2006).
[7] G. Martinellia, M. C. Carotta, M. Ferroni, Y. Sadaoka, E. Traversa, Sensors and Actuators B **55**, 99 (1999).
[8] G. A. Smolenskiiand, V. A. Bokov, Journal of Applied Physics **35**, 915 (1964).
[9] A. Scholl, J. Stohr, J. Luning, J. W. Seo, J. Fompeyrine, H. Siegwart, J.P. Locquet, F. Nolting, S. Anders, E. E. Fullerton, M. R. Scheinfein, H. A. Padmore, Science **287**, 1014 (2000).
[10] T. M. Rearick, G. L. Catchen, J. M. Adams, Physical Review B **48**, 224 (1993).
[11] S. E. Dann, D. B. Currie, M. T. Weller, M. F. Thomas, A. D. Al-Rawwas, Journal of Solid State Chemistry **109**, 134 (1994).
[12] W. C. Koehler, E. O. Wollan, Journal of Physics and Chemistry of Solids **2**, 100 (1957).
[13] S. Acharya, J. Mondal, S. Ghosh, S. K. Roy, P. Chakrabarti, Materials Letters **64**, 415 (2010).
[14] D.I. Khomskii, Journal of Magnetism and Magnetic Materials **306**, 1 (2006).
[15] J. W. Seo, E. E. Fullerton, F. Nolting, A. Scholl, J. Fompeyrine, J. P. Locquet, Journal of Physics: Condensed Matter **20**, 264014 (2008).
[16] G. R. Hearne, M. P. Pasternak, R. D. Taylor, P. Lacorre, Physical Review B **51**, 11495 (1995).
[17] E. V. Tsipis, E. A. Kiselev, V. A. Kolotygin, J. C. Waerenborgh, V. A. Cherepanov, V. V. Kharton, Solid State Ionics **179**, 2170 (2008).
[18] K. Iwasaki, T. Ito, M. Yoshino, T. Matsui, T. Nagasaki, Y. Arita, Journal of Alloys and Compounds **430**, 297 (2007).
[19] J. Joo, S. M Long, J. P Pouget, E. J Oh, A. G. MacDiamid, A. Epstain, Journal of Physical Review, 567 (1998).
[20] C. J. F. Buttcher, Theory of electrolytic polarisation. Amsterdam: Elsevier, (1952).